Low Temperature Physics/Fizika Nizkikh Temperatur, 2014, v. 40, No. 8, pp. 959–963

Low-temperature positron annihilation study of B^+-ion implanted PMMA

T.S. Kavetskyy[1], V.M. Tsmots[1], S.Ya. Voloshanska[1], O. Šauša[2], V.I. Nuzhdin[3], V.F. Valeev[3], Y.N. Osin[4], and A.L. Stepanov[3,4]

[1]*Drohobych Ivan Franko State Pedagogical University, 24 I. Franko Str., Drohobych 82100, Ukraine*
E-mail: kavetskyy@yahoo.com

[2]*Institute of Physics of Slovak Academy of Sciences, 9 Dúbravská cesta, Bratislava 84511, Slovakia*

[3]*Kazan Physical-Technical Institute of Russian Academy of Sciences, 10/7 Sibirskiy trakt, Kazan 420029, Russia*

[4]*Kazan Federal University, 18 Kremlyovska Str., Kazan 420008, Russia*

Received December 18, 2013, published online June 23, 2014

Temperature dependent positron annihilation lifetime spectroscopy (PALS) measurements in the range of 50–300 K are carried out to study positronium formation in 40 keV B^+-ion implanted polymethylmethacrylate (B:PMMA) with two ion doses of $3.13\cdot10^{15}$ and $3.75\cdot10^{16}$ ions/cm^2. The investigated samples show the various temperature trends of *ortho*-positronium (*o*-Ps) lifetime τ_3 and intensity I_3 in PMMA before and after ion implantation. Two transitions in the vicinity of ~150 and ~250 K, ascribed to γ and β transitions, respectively, are observed in the PMMA and B:PMMA samples in consistent with reference data for pristine sample. The obtained results are compared with room temperature PALS study of PMMA with different molecular weight (M_w) which known from literature. It is found that B^+-ion implantation leads to decreasing M_w in PMMA at lower ion dose. At higher ion dose the local destruction of polymeric structure follows to broadening of lifetime distribution (hole size distribution).

PACS: 81.05.Lg Polymers and plastics; rubber; synthetic and natural fibers; organometallic and organic materials;
78.70.Bj Positron annihilation;
61.80.Jh Ion radiation effects;
36.10.Dr Positronium.

Keywords: positron annihilation lifetime spectroscopy, positronium, ion implantation, polymethylmethacrylate, molecular weight.

1. Introduction

Ones of the most important materials for new generation nanoelectronics are polymer and copolymer systems. These materials are widely used for creation of polymeric nanomaterials (nanoparticles, nanocomposites, nanocrystals etc.) [1], polymer-quantum dot materials [2], copolymer-based nanomaterials (so-called “smart” nano-objects or ‘smart materials’) [3], nano-structured conducting polymers and polymer nanocomposites [4], photopolymerized tips for scanning-probe microscopy, a polymeric micropillar to evaluate mechanical properties [5], polymer electronic memories [6], copolymer systems to control inorganic-organic interfaces in fiber composites [7], polymer as gas sensors, pH sensors, ion-selective sensors, humidity sensors, biosensor devices [8] etc.

A lot of attempts were made by researches in the field of preparation, fabrication and design of polymer and copolymer materials, but the understanding structure-properties relationships and functionality of these materials is still required potential investigations. One of the important aspects to find such correlation can be resulted in more knowledge and better fundamental understanding of ion-irradiation (implantation) effects in polymers. Indeed, ion implantation of polymers is attractive as the effective technological method to turn dielectric polymers into conducting semiconductors [9]. A state-of-the-art review in the field of ion implantation of polymers has been done in the work [10].

One of the methods widely used to study structure-properties relationships in polymeric materials is positron annihilation lifetime spectroscopy (PALS) (see, for instance

[11–17] and references therein). The various important information on the positronium (Ps) formation (the electron-positron bound state) [18,19] in polymers can be extracted from PALS analysis. The present work is aimed to experimental study for the first time a positronium formation in B^+-ion implanted polymethylmethacrylate (B:PMMA) with energy of 40 keV and two ion doses of $3.13\cdot10^{15}$ and $3.75\cdot10^{16}$ ions/cm^2 using temperature dependent PALS measurements in the range of 50–300 K.

2. Experimental

As substrates for ion implantation, optically transparent 1.2-mm-thick PMMA plates were used. The B^+-ion implantation with energy of 40 keV, doses of $3.13\cdot10^{15}$ and $3.75\cdot10^{16}$ ions/cm^2 and ion current density < 2 μA/cm^2 was performed under a pressure of 10^{-5} Torr at room temperature on an ILU-3 ion accelerator at the Kazan Physical-Technical Institute (KPTI, Russia) [20].

Temperature dependent PALS measurements for the un-implanted PMMA and B:PMMA samples were carried out at the Institute of Physics of Slovak Academy of Sciences (IPSAS, Slovakia). The positron annihilation lifetime spectra were taken by the conventional fast-fast coincidence method using plastic scintillators coupled to photomultiplier tubes as detectors. The radioactive ^{22}Na positron source (1.5 MBq activity) was deposited in an envelope of Kapton foils and then sandwiched between two samples. This source-sample assembly was placed in a vacuum chamber between two detectors to acquire lifetime spectra at different temperatures. The time resolution (FWHM) of positron lifetime spectrometer was about 320 ps, measured by defect free Al sample as a standard. Analysis of lifetime spectra was carried out using the PATFIT-88/POSITRONFIT software package [21] with proper source corrections. Three component fitting procedure for PALS data treatment was applied, that gave the best fit, and long-lived lifetime component τ_3 and its intensity I_3, ascribing to the *ortho*-positronium (*o*-Ps) pick-off annihilation in free-volume spaces in accordance with the conventional interpretation [22], were finally taken into account for analysis.

The implanted PMMA samples were examined in the temperature range of 50–298 K using helium cryostat (Closed Cycle Refrigerator, Janis Research Company, Inc., USA) and vacuum equipment (Pfeiffer Vacuum, HiCUBE, Germany). The accuracy for the each selected temperature was ± 1 K and vacuum in the system was controlled within ~10^{-6}–10^{-7} mbar. The samples were measured in the cycles of heating and cooling. In the "heating" regime, the samples were fast cooled to 50 K and then measured from this temperature to 298 K with step of 20 K and elapsed time of 4–5 hours per point. In the "cooling" regime, the samples were measured from room temperature 298 K to 50 K with step of 20 K and elapsed time of 4–5 hours per point. At the selected temperatures the elapsed time was extended for better statistics in the lifetime spectra. For these temperatures the continuous lifetime analysis technique to obtain the distributions of *o*-Ps lifetime was employed, using MELT (maximum entropy lifetime) program [23].

3. Results and discussion

Figure 1 shows temperature dependence of the *o*-Ps lifetime τ_3 and intensity I_3 for the virgin PMMA sample. No significant hysteresis in $\tau_3(T)$ and $I_3(T)$ is observed within "heating" and "cooling" regimes. The numerical values of $\tau_3 \cong 1.85$ ns and intensity $I_3 \cong 26\%$ at room temperature are agreed well with those reported by Wang *et al.* [24]. As temperature decreases the τ_3 and I_3 go down showing changes in the vicinity of 150 and 250 K. The similar $\tau_3(T)$ and $I_3(T)$ trends in the range of 50–300 K with critical temperatures ~150 and ~250 K have also been detected for PMMA samples with different molecular weight (M_w) [25].

Moving from very low temperature to a higher temperature, the compression of molecules and structural transitions should be considered. The short review has been made by PerkinElmer [26] presenting the new PerkinElmer® DMA 8000 which allows accuracy and precision measurements of the transitions seen in thermoplastics,

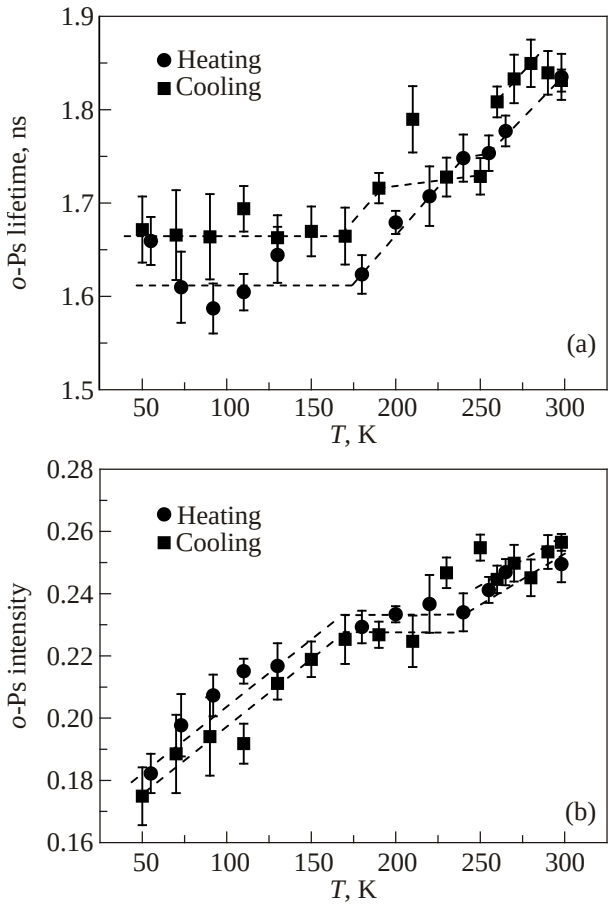

Fig. 1. The *o*-Ps lifetime τ_3 (a) and intensity I_3 (b) versus temperature for PMMA. The dashed lines are drawn as a guide for the eye.

caused by molecular motions and free volume changes defining how a polymer will behave at a certain temperature. The compression of polymer matrix at low temperature is limited to inter- and intramolecular motions within the scale of a single repeat unit [26] and could be called by two mechanisms: (i) the intermolecular compression or compression between molecular chains of polymer; and (ii) the intramolecular compression or compression between molecules of polymer. The inter- and intramolecular compression is ascribed to gamma transition, T_γ, as a starting transition at low temperature when localized bond movements (bending and stretching) and side chain movements can occur in polymers. As the temperature and free volume increases the beta transition, T_β, is considered to be often related to the toughness or material properties in the glassy state. This transition is also called as the sub-glass transition, sub-T_g (or sub-alpha transition, sub-T_α) or the T_g of a secondary component in a blend or of a specific block in a block copolymer [26].

Low temperature positron studies in PMMA [25] are found to be sensitive to these structural transitions showing that two transitions corresponding to the temperatures of ~150 and ~250 K can be ascribed to γ and β transitions respectively. The temperature 250 K for PMMA has also been denoted as the secondary transition temperature T_β [24]. Thus, the threshold temperatures of ~150 and ~250 K detected for the un-implanted PMMA in this work (Fig. 1) are related to the T_γ and T_β respectively, as well.

Figure 2 presents the $\tau_3(T)$ and $I_3(T)$ behavior after B^+-ion implantation of the PMMA with lower ion dose of $3.13\cdot10^{15}$ ions/cm^2. In this case an overlapping the contributions from the bulk PMMA matrix and the thin implanted layer seems to be worked. The thresholds temperatures of ~150 and ~250 K are ascribed to γ and β transitions respectively as mentioned above. In the range of 150–250 K the $\tau_3(T)$ character is likely to hysteresis curve. At the same time, no significant difference in the τ_3 magnitude (or size of voids of radius R within the well-known semiempirical τ_3-R equation in a spherical infinitive potential model [27–29]) is detected for the B:PMMA at ion dose of $3.13\cdot10^{15}$ ions/cm^2 compared to the pristine sample as well as the intensity I_3 magnitude (proportional to *o*-Ps probability). But, in contrast to the pristine sample, the $I_3(T)$ shows linear character in the whole temperature range studied.

Figure 3 demonstrates the $\tau_3(T)$ and $I_3(T)$ behavior after B^+-ion implantation of the PMMA with higher ion dose of $3.75\cdot10^{16}$ ions/cm^2. Here the sample should be considered

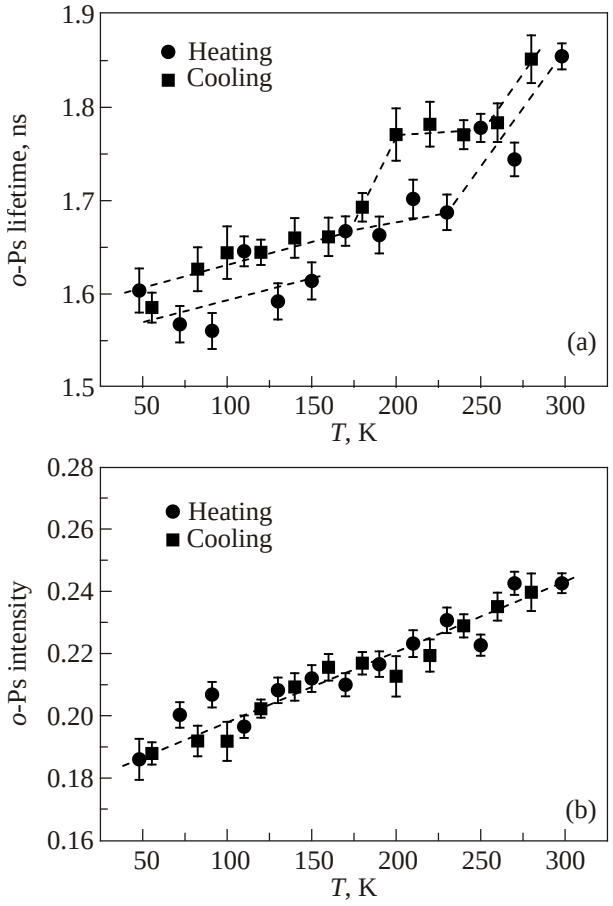

Fig. 2. The *o*-Ps lifetime τ_3 (a) and intensity I_3 (b) versus temperature for B:PMMA with ion dose of $3.13\cdot10^{15}$ ions/cm^2. The dashed lines are drawn as a guide for the eye.

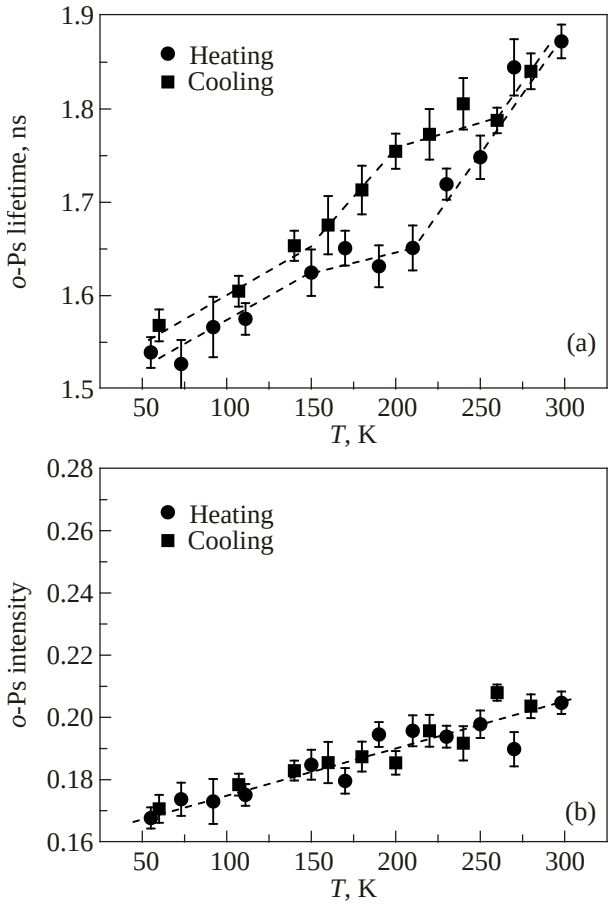

Fig. 3. The *o*-Ps lifetime τ_3 (a) and intensity I_3 (b) versus temperature for B:PMMA with ion dose of $3.75\cdot10^{16}$ ions/cm^2. The dashed lines are drawn as a guide for the eye.

as the heterostructure of three phases: (i) the implanted layer involving the damaged PMMA regions, (ii) the carbon clusters forming the carbon layer, and (iii) the PMMA matrix as the substrate. The wider hysteresis on the $\tau_3(T)$ in the range of T_γ (~150 K) and T_β (~250 K) is observed in this case as ion dose increases; the $I_3(T)$ dependence is linear. At low temperatures, below 150 K, a slight reduction of τ_3 magnitude (or size of voids) compared to the pristine sample is found out, while the intensity I_3 decreases more significantly in the whole temperature range of 50–300 K. The latter could be explained as a signature on the different compression of voids in the carbon clusters and the pure PMMA matrix.

It should be noted here that distributions of *o*-Ps lifetime (or voids) estimated by MELT program testify on the changes in the M_w of polymer [30]. Figure 4 shows the *o*-Ps lifetime distribution at different temperatures in PMMA and B:PMMA with ion dose of $3.13{\cdot}10^{15}$ ions/cm^2. The agreement between *o*-Ps lifetime distributions at room temperature after cycle of fast cooling and heating is clearly seen indicating the reproducibility of the simulation performed. The *o*-Ps lifetime data obtained with POSITRONFIT (Figs. 1 and 2) and with MELT (Fig. 4) are also agreed well. The *o*-Ps relative intensity of MELT as a function of temperature is found to be non-linear for the pristine sample and linear for the irradiated sample in consistence with the *o*-Ps probability trends exemplified by $I_3(T)$.

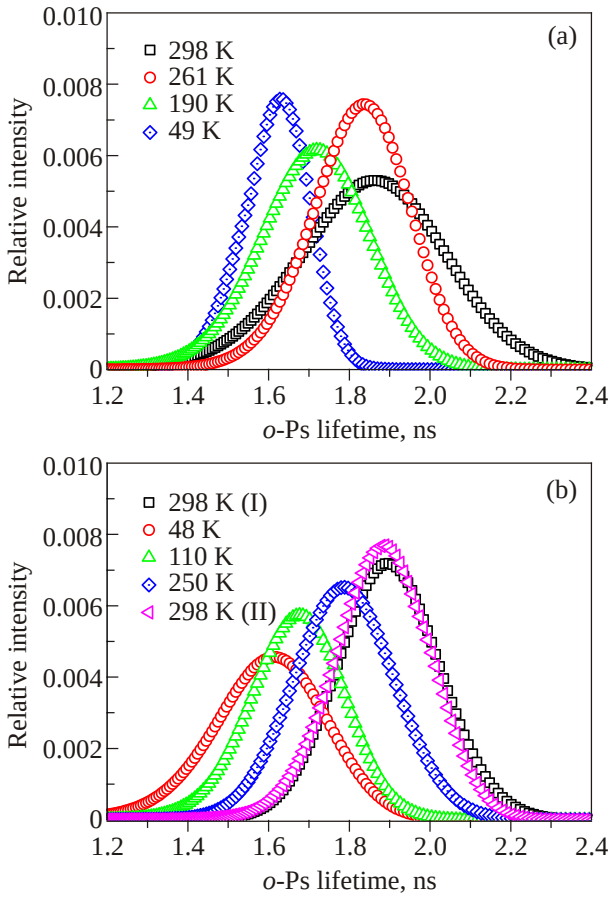

Fig. 4. (Color online) The *o*-Ps lifetime distribution at different temperatures in PMMA (a) and B:PMMA with ion dose of $3.13{\cdot}10^{15}$ ions/cm^2 (b). The temperature 298 K (I) stands for a start point, while the temperature 298 K (II) is attained after cycle of fast cooling and heating. The agreement between *o*-Ps lifetime distributions for 298 K (I) and 298 K (II) is seen.

Figure 5 illustrates the *o*-Ps lifetime distributions in the B:PMMA at two different ion doses ($3.13{\cdot}10^{15}$ and $3.75{\cdot}10^{16}$ ions/cm^2) and temperature ~300 K. It should be noted here that He *et al*. [30] showed that *o*-Ps lifetime distributions (or the distribution of free volume detected by *o*-Ps) are broadening with the increase of M_w in the PMMA. The explanation of this finding has been made on the assumption that fast motion is dependent on M_w in high molecular weight linear polymer because of the coupling between fast motion and segmental mobility. As the authors [30] considered, in a higher molecular weight polymer some fast motions may be inhibited or change to slow mode due to stronger intermolecular interactions, resulting in the *o*-Ps localization in a smaller free volume and a larger hole and, consequently, a wider *o*-Ps lifetime distribution and more holes are detected by *o*-Ps.

According to these observations [30], it is found out in our case that B^+-ion implantation into PMMA leads to decreasing M_w in polymer at lower ion dose ($3.13{\cdot}10^{15}$ ions/cm^2) because of the narrowing the *o*-Ps lifetime distribution. The broadening the *o*-Ps lifetime distribution at ~300 K in polymer at higher ion dose ($3.75{\cdot}10^{16}$ ions/cm^2) is probably connected with local destroying of polymeric structure and with generation of additional free volume holes (with different hole sizes) rather than with the increasing M_w, as we suggest.

As above mentioned fast motion has molecular weight dependence from coupling model with β-process assumed by the authors [30], the our experimental finding on the *o*-Ps lifetime distribution in B:PMMA at ion dose of $3.13{\cdot}10^{15}$ ions/cm^2 might be understood as the weaker intermolecular interactions and the *o*-Ps localization in a

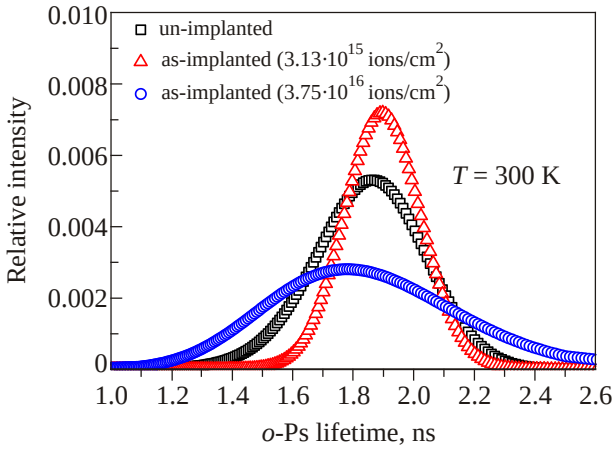

Fig. 5. (Color online) The *o*-Ps lifetime distributions in B:PMMA at different ion doses at temperature ~300 K.

larger free volume and a smaller hole. It should be mentioned that the secondary glass transition T_β occurs at ~250 K far below the glass transition T_g = (355 ± 18) K of PMMA [24] and, thus, it is rational indeed that *o*-Ps lifetime distribution is considered within the β-process of the mode-coupling theory.

Finally, the origin of the observed hysteresis of $\tau_3(T)$ in the range of 150–250 K after B^+-ion implantation of the PMMA with lower (< 10^{16} ions/cm^2) and higher (> 10^{16} ions/cm^2) ion doses and changes of molecular weight is not fully understood yet. The uncontrolled impact (if any) of positron irradiation during PALS measurements and ion current density during ion implantation on the B:PMMA structure should be examined. Such experiments will be further performed.

4. Conclusions

In the present work temperature dependent PALS measurements in the range of 50–300 K have been carried out to study positronium formation in the 40 keV B:PMMA with two ion doses of $3.13\cdot10^{15}$ and $3.75\cdot10^{16}$ ions/cm^2. The investigated samples showed the various temperature trends of *o*-Ps lifetime τ_3 and intensity I_3 in the PMMA before and after ion implantation. Two transitions in the vicinity of ~150 and ~250 K, ascribed to γ and β transitions, respectively, have been observed in the PMMA and B:PMMA samples. The obtained results have been compared with room temperature PALS study of PMMA with different molecular weight, M_w. It is found that B^+-ion implantation leads to decreasing M_w in PMMA at lower ion dose. At higher ion dose the broadening the lifetime distribution is probably caused by local destruction of PMMA matrix and generation of additional free volumes.

Acknowledgements

T.S. Kavetskyy and A.L. Stepanov acknowledge the SAIA for scholarships within the National Scholarship Programme of the Slovak Republic. O. Šauša wishes to thank the Slovak Grant Agency VEGA for support by the grant No. 2/0099/10 and Agency ME SR for Structural Funds EU (Cekomat II, ITMS 2624012002102). This work was also partly supported by the SFFR of Ukraine No. F52.2/003 and the RFBR Nos. 13–02–12012, 12–02–00528 and 12–02–97029 in Russia.

1. A.P. Kumar, D. Depan, N.S. Tomer, and R.P. Singh, *Prog. Polym. Sci.* **34**, 479 (2009).
2. N. Tomczak, D. Jańczewski, M. Han, and G.J. Vancso, *Prog. Polym. Sci.* **34**, 393 (2009).
3. J. Rodríguez-Hernández, F. Chécot, Y. Gnanou, and S. Lecommandoux, *Prog. Polym. Sci.* **30**, 691 (2005).
4. Rajesh, T. Ahuja, and D. Kumar, *Sens. Actuators B* **136**, 275 (2009).
5. K.-S. Lee, R.H. Kim, D.-Y. Yang, and S.H. Park, *Prog. Polym. Sci.* **33**, 631 (2008).
6. Q.-D. Ling, D.-J. Liaw, C. Zhu, D.S.-H. Chan, E.-T. Kang, and K.-G. Neoh, *Prog. Polym. Sci.* **33**, 917 (2008).
7. H.G. Borner, *Prog. Polym. Sci.* **34**, 811 (2009).
8. B. Adhikari and S. Majumdar, *Prog. Polym. Sci.* **29**, 699 (2004).
9. D.V. Sviridov, *Russ. Chem. Rev.* **71**, 315 (2002).
10. V.N. Popok, *Rev. Adv. Mater. Sci.* **30**, 1 (2012).
11. E. Zengeni, P.C. Hartmann, R.D. Sanderson, and P.E. Mallon, *J. Appl. Polym. Sci.* **119**, 1060 (2011).
12. M.M. Feldstein, E.V. Bermesheva, Y.C. Jean, G.P. Misra, and R.A. Siegel, *J. Appl. Polym. Sci.* **119**, 2408 (2011).
13. M. Zeng, C. Lu, B. Wang, and C. Qi, *Radiat. Phys. Chem.* **79**, 966 (2010).
14. S. Zhang, K.Y. Wang, T.-S. Chung, H. Chen, Y.C. Jean, and G. Amy, *J. Membr. Sci.* **360**, 522 (2010).
15. J. Wang, J. Gong, Z. Gong, X. Yan, B. Wang, Q. Wu, and S. Li, *Nucl. Instrum. Meth. Phys. Res. B* **268**, 2355 (2010).
16. H. Wu, W. Hou, J. Wang, L. Xiao, and Z. Jiang, *J. Power Sources* **195**, 4104 (2010).
17. Y. Shibahara, H.S. Sodayea, Y. Akiyama, S. Nishijima, Y. Honda, G. Isoyama, and S. Tagawa, *J. Power Sources* **195**, 5934 (2010).
18. *Positron Spectroscopy of Solids, Proceedings of the International School of Physics "Enrico Fermi", Course CXXV*, A. Dupasquier and A.P. Mills, Jr. (eds.), Washington DC (1995).
19. C. He, S. Wang, Y. Kobayashi, T. Ohdaira, and R. Suzuki, *Phys. Rev. B* **86**, 075415 (2012).
20. A.L. Stepanov, *Tech. Phys.* **49**, 143 (2004).
21. P. Kirkegaard, M. Eldrup, O.E. Mogensen, and N.J. Pedersen, *Comp. Phys. Commun.* **23**, 307 (1981).
22. *Positron and Positronium Chemistry: Studies in Physics and Theoretical Chemistry*, D.M. Shrader and Y.C. Jean (eds.), Elsevier, New York (1988).
23. A. Shukla, M. Peter, and L. Hoffmann, *Nucl. Instr. Meth. A* **335**, 310 (1993); L. Hoffmann, A. Shukla, M. Peter, B. Barbiellini, and A.A. Manuel, *ibid*. **335**, 276 (1993).
24. C.L. Wang, T. Hirade, F.H.J. Maurer, M. Eldrup, and N.J. Pedersen, *J. Chem. Phys.* **108**, 4654 (1998).
25. M. Tashiro, P.K. Pujari, C.Y. Tseng, S. Seki, Y. Honda, and S. Tagawa, *Hoshasen Kagaku Toronkai Koen Yoshishu* **43**, 188 (2000); P.K. Pujari, M. Tashiro, C.Y. Tseng, Y. Honda, S. Nishijima, and S. Tagawa, *Mater. Sci. Forum* **363–365**, 275 (2001).
26. www.perkinelmer.com (Dynamic Mechanical Analysis Basics: Part 2 Thermoplastic Transitions and Properties).
27. S.J. Tao, *J. Chem. Phys.* **56**, 5449 (1972).
28. M. Eldrup, D. Lightbody, and J.N. Sherwood, *Chem. Phys.* **63**, 51 (1981).
29. N. Nakanishi, S.J. Wang, and Y.C. Jean, in: *International Symposium on Positron Annihilation Studies of Fluids*, S.C. Sharma (ed.), World Scientific, Singapore (1988), p. 292.
30. C.Q. He, Y.Q. Dai, B. Wang, and S.J. Wang, *Mater. Sci. Forum* **363–365**, 309 (2001).